Title: Hippocampal place cell encoding of sloping terrain

Abbreviated title (60 char): Hippocampal place cell encoding of sloping terrain

Authors: Porter, Blake S.[1,2] Schmidt, Robert [3] & Bilkey, David K. [1,2]

[1] Department of Psychology, University of Otago, Dunedin, NZ, 9016

[2] Brain Health Research Centre, University of Otago, Dunedin, NZ, 9016

[3] Department of Psychology, the University of Sheffield, Sheffield, UK, S1 2LT

Number of Pages: 45

Number of Figures: 6

Number of Tables: 3

Corresponding Author: Blake S. Porter. 275 Leith Walk, Department of Psychology, University of Otago, Dunedin, NZ, 9016. blakeporterneuro@gmail.com

Grant sponsor: The Royal Society of New Zealand Marsden Fund

Grant number: UOO1212

Contributions: B.S.P and D.K.B. designed the experiments. B.S.P performed the experiments. B.S.P and D.K.B analyzed the data. B.S.P, R.S., and D.K.B interpreted the results and wrote the paper

Abstract

Effective navigation relies on knowledge of one's environment. A challenge to effective navigation is accounting for the time and energy costs of routes. Irregular terrain in ecological environments poses a difficult navigational problem as organisms ought to avoid effortful slopes to minimize travel costs. Route planning and navigation have previously been shown to involve hippocampal place cells and their ability to encode and store information about an organism's environment. However, little is known about how place cells may encode the slope of space and associated energy costs as experiments are traditionally carried out in flat, horizontal environments. We set out to investigate how dorsal-CA1 place cells in rats encode systematic changes to the slope of an environment by tilting a shuttle box from flat to 15° and 25° while minimizing external cue change. Overall, place cell encoding of tilted space was as robust as their encoding of flat ground as measured by traditional place cell metrics such as firing rates, spatial information, coherence, and field size. A large majority of place cells did, however, respond to slope by undergoing partial, complex remapping when the environment was shifted from one tilt angle to another. The propensity for place cells to remap did not, however, depend on the vertical distance the field shifted. Changes in slope also altered the temporal coding of information as measured by the rate of theta phase precession of place cell spikes, which decreased with increasing tilt angles. Together these observations indicate that place cells are sensitive to relatively small changes in terrain slope and that terrain slope may be an important source of information for organizing place cell ensembles. The terrain slope information encoded by place cells could be utilized by efferent regions to determine energetically advantageous routes to goal locations.

Introduction

Navigation that accounts for the energetically-demanding aspects of terrain topology has the potential to save an organism a great deal of time and energy compared to that which only considers the distance to a goal. In practical terms this is instantiated in the empirically validated (Scarf, 2007), century old, Naismith's rule (Naismith, 1892) for planning hiking routes: Account for one hour for every three miles (4,828 meters) on flat terrain and one additional hour for every 2,000 feet (610 meters) of ascent. Over and above the costs associated with the extra time, humans (Hoogkamer, Taboga, & Kram, 2014; Margaria, Cerretelli, Aghemo, & Sassi, 1963; Minetti, Moia, Roi, Susta, & Ferretti, 2002) and rodents (Armstrong, Laughlin, Rome, & Taylor, 1983; Brooks & White, 1978; Chavanelle et al., 2014) expend significantly more energy when travelling on inclined surfaces compared to travelling on flat ground. Many other species, including elephants (Wall, Douglas-Hamilton, & Vollrath, 2006) and monkeys (Di Fiore & Suarez, 2007) appear to factor in these time and energy costs when navigating, as they avoid traversing over hills in their natural habits when alternatives are available. In particular, monkeys will travel along energetically advantageous "highways" year after year, suggesting that they possess a representation of the environment that includes the effort demands of routes (Di Fiore & Suarez, 2007). However, while topology-related factors clearly influence navigation, it is not clear how the brain represents the potentially costly three-dimensional (3D) nature of ecological environments (Jeffery, Jovalekic, Verriotis, & Hayman, 2013).

Place cells (O'Keefe & Dostrovsky, 1971; O'Keefe & Nadel, 1978) are hippocampal neurons that appear to have a role in representing the spatial environment. These cells are active at a specific location in an environment such that an ensemble of many place cells will encode an entire region as well as many features of that environment (for review; Eichenbaum, 2004). A diverse range of external sensory inputs have been shown to modulate

and drive the selective firing of place cells such as environmental contexts (Muller & Kubie, 1987; Smith & Mizumori, 2006), landmarks (Gothard, Skaggs, Moore, & McNaughton, 1996; Knierim, Kudrimoti, & McNaughton, 1998), objects (Komorowski, Manns, & Eichenbaum, 2009; McKenzie, Frank, Kinsky, Porter, Rivière, et al., 2014), and odors (Jeffery & Anderson, 2003). The vestibular system also has a part to play as lesions of this region abolish the spatial selectivity of place cells (Russell, Horii, Smith, Darlington, & Bilkey, 2003;. Stackman, Clark, & Taube, 2002) as well as impair spatial memory and navigation (Smith, 1997; Smith et al., 2005). These findings suggest that self-motion (Wallace, Hines, Pellis, & Whishaw, 2002), gravitational, and head/ body orientation (Stackman & Taube, 1997; Taube, 1998) information provided by the vestibular system are vital to a place cell's functionality and the neural representation of space.

As a result of their vestibular inputs, place cells may be especially attuned to gravitational and head/body orientation information which may allow them to encode the topology space. Previous studies have, for example, shown that place cell activity is sensitive to changes in slope. For example, when half of a rectangular track was tilted (Knierim & McNaughton, 2001), some place cells altered their activity by firing in a different location or shutting off all together with new place cells becoming active; a phenomenon known as "remapping". In a separate study (Jeffery, Anand, & Anderson, 2006) it was shown that the rotation of a tilted open field caused the ensemble of place cells that represented the field to shift their fields in relation to the rotation, indicating that the cells were sensitive to the slope direction.

Despite these findings, it remains unclear how place cells, and ultimately the cognitive maps that might be used for navigation, encode terrain slope. Previous experiments investigating this question (Jeffery et al., 2006; Knierim & McNaughton, 2001) used steep slope angles which did not allow for the full investigation of the cell's sensitivity to terrain

slope; are place cells responsive to small changes in slope angle or do they require a substantial slope to alter their firing patterns? Furthermore, the latter study (Knierim and McNaughton, 2001) is the only previous investigation where the slope of the environment was changed systematically. Unfortunately, in this previous experiment changes to the tilt of the apparatus were accompanied by changes to the rat's view of the external environment which may have confounded any effects observed.

More generally, debate continues as to whether or not land travelling mammals encode the vertical axis of space (Taube & Shinder, 2013). One proposal is that encoding of height within a cognitive map is minimal (Hayman, Verriotis, Jovalekic, Fenton, & Jeffery, 2011) and that multiple planar maps are used to represent each surface which are then pieced together to encode 3D space (Jeffery et al., 2013). Alternatively, it has been proposed that mammalian brains may be capable of encoding space in different ways depending on the environment and how an organism travels through it (Savelli & Knierim, 2011; Ulanovsky, 2011). For example, surface locomotion may result in the generation and use of anisotropic (vertical space is encoded differently than horizontal space) planar maps (Ulanovsky & Moss, 2007) while flying results in the use of isotropic (horizontal and vertical space are encoded in the same manner) volumetric maps (Finkelstein et al., 2014; Yartsev & Ulanovsky, 2013).

In the present experiment we set out to gain a better understanding of how rodent place cells respond to and represent tilted surfaces and in doing so to shed light on how cognitive maps encode three-dimensional space. We recorded place cells from dorsal CA1 as rats ran back and forth on a cue-devoid linear track which could either lie flat (0°) or be tilted to 15° and 25°. Our data show that place cells were sensitive to as little as 10° (15° to 25°) changes in tilt and partial remapping was observed between all tilt conditions. Furthermore, the amount of remapping observed was positively correlated with how different the angle was between any two conditions. Nonetheless, a subgroup of place cells also remained stable

across tilt conditions, continuing to represent a location on the track, irrespective of slope. Together, these data suggest that the firing of a subpopulation of place cells is modulated by the slope of an environment with individual place cells having different levels of sensitivity to slope angle. We also provide further evidence that the rat, a land-travelling mammal, utilizes an anisotropic encoding scheme for representing 3D space.

Materials and Methods

Subjects

Seven male Sprague Dawley rats were aged between 4-6 months old and weighed between 350-500 grams were obtained from the University of Otago's Hercus-Taieri Resource Unit. Upon arrival rats were housed in groups of three. Grouped rats were housed in plastic cages with wire metal lids (40 x 55 x 27 cm). The animal housing room was maintained at a 12 hour light/dark cycle and kept between 20-22 °C. Rats were given two weeks from the time of arrival to acclimate to the new facility where they had *ad libitum* access to food (18% Protein Rodent Diet, Teklad Global Inc.) and water. After two weeks, rats were food deprived to no less than 85% of their free-feeding weight to stimulate interest in the food reward (Coco Pops cereal, Kellogg Company) used for training and given in the experimental phase. Water continued to be available *ad libitum* throughout the study. All experimentation was done during the light phase.

Apparatus

The experiment was conducted in a wooden shuttle box measuring 120 cm long by 24 cm wide with 60 cm tall walls. The entire apparatus was painted matte black and was devoid of any visual cues. The floor was a matte black rubber mat with a diamond pattern to provide the animals with grip while running. At each end of the shuttle box was a matte black plastic semi-circular well where the food reward (Coco Pops) was dispensed. The Coco Pops were

delivered through a PVC tube so that the experimenter could unobtrusively provide the rat with a food reward without interfering with cues inside the box.

The apparatus could be laid flat on the ground so that the floor of it was horizontal (0°), and also tilted to two different inclines, 15° and 25° (Fig. 1a). A camera was used to record the position of the rat based on infrared LEDs fixed to the data acquisition system's headstage. This camera was mounted to the apparatus at its midpoint so that its field of view of the maze remained constant when the apparatus was tilted. In order to minimize any extra-maze cues, the only source of light in the room was a computer monitor 2.3 meters away from the apparatus. The monitor's brightness was dimmed as low as possible. All other sources of light in the room were covered including the LEDs on equipment and the door jambs. Furthermore, the wall closest to the apparatus was painted matte black, as seen in Fig 1a. The two walls perpendicular to the apparatus, the only two possibly viewable by the rats when the apparatus was tilted, were both over a meter away and devoid of any cues. Because of the measures that were used to minimize extra-maze cues, combined with the known poor visual acuity of albino rats (Pursky *et al.*, 2002), it is extremely unlikely the rats could detect any visual changes associated with tilt.

Preoperative training

During the first five days of preoperative training, rats were familiarized to the recording room, experimenter, and apparatus. Rats were placed in the experimental apparatus and allowed to free forage for Coco Pops randomly scattered throughout. Once rats were readily foraging in the apparatus they were encouraged to shuttle between the two endzones by making Coco Pops only available at either end. When rats were readily shuttling while the apparatus was at 0° we began to tilt the apparatus. Initially, rats were allowed to shuttle for five minutes with the apparatus at 0° and given two Coco Pops upon arrival at the endzone.

The apparatus was then tilted to 15° with the rat still in the apparatus. The rat then shuttled at 15° for five minutes for the same reward amount. Following this, the apparatus was tilted to 25° and the rat shuttled for a third five minute session with the same reward amount. Each day the side of the apparatus which was elevated was alternated. Some rats shuttled in the tilted conditions on the first day of exposure while others took up to seven days to shuttle in all tilt conditions. Once a rat was shuttling for five minutes in each condition, a lap count measure of performance was utilized. A lap consisted of the rats running from one endzone to the opposite endzone and then back. Rats were trained each day until they were readily shuttling for 20 laps in each of the three tilt conditions. It took an average of two days for rats to reach the 20 lap criterion. All rats were then run on the 20 lap per condition sequence for at least one week to ensure consistent behavior (no stopping or turning around during a lap). At this point rats were ready to be implanted with microdrives.

Surgery

All experimental protocols were approved by the University of Otago Animal Ethics Committee and conducted in accordance with New Zealand animal welfare legislation. Anaesthesia was induced through 5% isoflurane (Merial New Zealand, Ltd.) in oxygen and maintained at 2-2.5% during surgery. Once induced, animals were given the analgesics Carprofen (a non-steroidal anti-inflammatory drug, 1mg/kg) and Temgesic (buprenorphine, 0.33mg/kg) as well as a prophylactic antibiotic, Amphoprim (trimethoprim and sulphamethazine, 0.2ml,) before being placed into a stereotaxic frame with non-puncture ear bars (David Kopf Instruments, Inc.). The scalp was shaved and sterilized with Betadine (Povidone-iodine) followed by a subcutaneous injection of Lopaine (lignocaine hydrochloride 20mg/ml; 0.1ml diluted in 0.4ml of sterile saline) as a local anesthetic in the scalp.

Six rats were implanted with 8-channel Scribe microdrives (Bilkey & Muir, 1999) and one rat was implanted with a custom 64-channel microdrive array. The electrodes of all drives were prepared as tetrodes (four electrodes tightly spun and heated together); two tetrodes for the 8-channel drive and 15 for the 64-channel drive. Electrodes consisted of 25 µm nichrome, heavy formvar insulated wire (Stablohm 675 HFV NATRL; California Fine Wire Company) for Scribe microdrives. For the 64-channel microdrive array, the electrodes were made from 17.5 µm platinum 10% iridium, polymide insulated wire (California Fine Wire Company). All electrodes were gold (nichrome) or platinum (platinum 10% iridium) electroplated to reduce their impedances to between 200-250 kΩ (NanoZ; Neuralynx, Inc.). Tetrodes were stereotaxically targeted at the dorsal aspect of the hippocampal CA1 subregion of the right hemisphere (anteroposterior, -3.7 mm; mediolateral, +2.2 mm (Paxinos & Watson, 2007)). Tetrodes were lowered approximately 1.5 mm from the dura into the brain. Rats were also implanted with a single local field potential (LFP) electrode (200 µm thick insulated nichrome wire; Johnson Matthey, Inc.) into the ACC (anteroposterior, +2.0 mm; mediolateral, +0.4 mm). The ACC LFP data is not presented in this paper. A skull screw over the cerebellum served as a ground connection. Post-surgery rats received secondary doses of Temgesic, Carprofen, and Amphoprim. Rats were given 10 days to recover before behavioral testing resumed.

Postoperative training

Postoperative training was carried out to ensure rats could still perform the task adequately, adjust to their implant, and to optimize electrode placement. Rats' food was again reduced to maintain 85% of their free feeding weight. For each day of postoperative training rats were plugged into the data acquisition system's tethered headstage. On the first day of postoperative training, Coco Pops were randomly placed within the apparatus and the rat was given 15 minutes to forage freely to adjust to the weight of their implant. On subsequent

days, rats shuttled for 20 laps on each tilt condition, 0°, 15°, and 25°, counterbalancing for which end of the apparatus was elevated. Nearly all rats were able to carry this out on the first day. However, a few rats took between three to five days to acclimate to their implants and carry out all 60 laps. All rats had a minimum of seven sessions of postoperative training (20 laps per condition) prior to starting the experimental protocol.

Electrophysiological recordings

During postoperative training single unit and local field potential (LFP) data were closely monitored. Tetrodes were lowered towards dorsal CA1 (dCA1) over the course of two to four weeks until well isolated single units were identified. During this period rats were running the postoperative training outlined above. Neurophysiological and animal movement data were acquired with an Axona multichannel data acquisition system (DacqUSB; Axona, Ltd.) for both the 8- and 64- channel microdrives. Single unit data was bandpass filtered between 600 and 6,000 Hz and digitized at 48 kHz. Signals were amplified between 5,000 and 9,000 times. For each tetrode, one electrode with minimal spiking activity on a different tetrode served as a reference. Action potentials were detected by threshold crossing of approximately 70 μV. LFP data was sampled at 4,800 Hz and bandpass filtered between 1 and 500 Hz.

Experimental protocol

Once dCA1 single units were being consistently obtained day to day the experimental sequence began. The experimental sequence consisted of six recording sessions, one per day for six days. Each day rats consecutively ran ~20 laps in each of the three tilt conditions, 0° flat, 15° tilt, and 25° tilt. One lap consisted of the rat running from one end of the shuttle box to the other, consuming the reward at the endzone, and returning to the start endzone to consume its reward. After ~20 laps under one condition, the rat remained in the apparatus and

ran one more lap while the apparatus was tilted to the next condition. Tilt condition presentation order was counterbalanced across days such that no condition was experienced in the same order position (Fig. 1c) and for the first three days the north endzone was elevated, while for the second three days the south endzone was elevated.

During the experimental sequence tetrodes were not manipulated. Three rats were run on the whole experimental sequence once while three were run on it twice with at least a two day break in between data collection. In between the two six day data collection sequences tetrodes were manipulated in order to obtain recordings from new single units. Tetrodes were lowered approximately 40-80 μm per day until new units were obtained (visual inspection of waveforms online and offline) or until the tetrodes moved out of the dCA1 layer.

Analysis

For each recording, single units were manually isolated offline in Offline Sorter (Version 3; Plexon, Inc.) primarily using peak-to-valley distance and principal components analysis of the waveforms. The single unit spiking data was then exported to Matlab along with the behavioral tracking data. All data analysis was carried out using Matlab with native and custom written scripts. All measurements are stated as means ± standard error of the mean.

Behavior analysis

The apparatus was broken up into two regions of interest (ROIs); running and endzones (Fig. 1b). The endzones consisted of the two ends of the shuttle box where the reward was dispensed and consumed. The area in between the two endzone boundaries (103 cm long) was considered the running ROI where rats were actively shuttling between endzones. All analysis reported here was restricted to the running ROI. One trial counted as the rat running from the boundary of one endzone to the boundary of the opposite endzone

(half a lap). Trials where the rat did not complete the end to end run were excluded. Failed shuttles were, however, quite rare, typically occurring on only one to two trials per condition. Trials where the rat took longer than 7 seconds to shuttle (had an average speed below 15 cm/s) were also excluded to keep trial-to-trial speeds consistent. A trial's slope direction was determined to be uphill or downhill based on which endzone the rat departed from. Trials where the rat originated from the endzone on the ground and shuttled to the elevated endzone were considered uphill and vice versa for downhill. For the non-tilt (0°) condition, "uphill" and "downhill" trials correspond to the same running direction in relation to the tilted conditions occurring during that session.

Single unit analysis

For every single unit, the firing rate of each trial was determined by the duration of the trial and the number of spikes that cell fired during that trial. Condition (tilt by slope direction) firing rates were determined by dividing total trial durations for that condition by the number of spikes that occurred in that condition. All analyses were restricted to cells categorized as place cells. To be considered a place cell, single units had to have discharged at least 100 spikes and to have a mean firing rate of at least 0.1 Hz for at least one of the six possible conditions (three tilt, 0°, 15°, 25°; two slope directions, uphill and downhill). In addition, a place cell had to have a spatial information score (see below) of at least 1 bit/spike and spatial coherence (see below) greater than 0.5 for at least one condition. Data was pooled across animals, however, the general patterns described were consistent across all animals tested.

Place cell metrics

In order to determine the peak firing rate and place field size, the floor of the shuttle box was subdivided into 2.5cm^2 bins. An occupancy map based on the tracking data was then

created based on the amount of time the rat spent in each bin. Bins with an occupancy time less than 100 milliseconds were removed. A spike map was then created for each single unit based on the number of spikes which occurred in each bin. Elementwise division was used between the spike map and occupancy map to create a firing rate map where each bin contained the firing rate for a cell. The peak firing rate for a place cell was determined by the bin which had the highest firing rate.

A place field map was created for each cell based on the firing rate map. Place field maps utilized a firing rate criterion to remove bins where the cell was not substantially active in and/or did not display place field-like activity. First, a Gaussian smoothing kernel was applied to the firing rate map with a $2.5cm^2$ (1 sigma) smoothing window. Following this, each bin of the place field map was checked to see if it had a firing rate of at least 15% of the peak firing rate and had seven neighboring bins that also met this firing rate criterion. If a bin did not meet these criteria it was set to 0 on the place field map so it would not be included in the place field size calculation. Following this process of removing underactive bins, the number of distinct place fields was found using Matlab's bwlabel function for finding connected components. Afterwards, each field was analyzed separately for its size (total bins with elevated firing), length, width, and aspect ratio (length/width). If a place cell had multiple fields, we chose the largest field to be its "main field". All further place cell analysis described below was carried out on the unsmoothed firing rate maps (not the place field maps).

Spatial information measures the amount of information, in bits per spike, that a given spike conveys about the rat's location within an environment (Skaggs, Mcnaughton, Gothard, & Markus, 1993). The more spatial information a cell's spikes convey, the more that cell can be relied upon to decode the rat's position within the environment. The formula for spatial information is as follows:

$$Information = \sum_{i=1}^{N} p_i \frac{\lambda_i}{\lambda} \quad log2 \frac{\lambda_i}{\lambda}$$

where the environment is divided into N non-overlapping bins with i =1,…, N, p_i is the occupancy probability of bin i, λ_i is the mean firing rate for bin i, and λ is the overall mean firing rate of the neuron.

Sparsity was also measured for each place cell (Skaggs, McNaughton, Wilson, & Barnes, 1996). Sparsity is akin to information in that it measures the portion of the environment in which a cell is active. The formula for sparsity is:

$$Sparsity = \frac{[\lambda]}{[\lambda^2]} = \frac{(\sum p_i \lambda_i)^2}{\sum p_i \lambda_i^2}$$

where the square brackets [ ] denote the expected value average over all locations. All other symbols are as described for the *Information* equation.

Spatial coherence is a measure of how spatially concentrated a place cell's activity is (Muller & Kubie, 1989). Spatial coherence is measured by the average z-transformed correlation of the firing rate of a given bin to the mean firing rate of the surrounding eight bins, carried out for every bin of the apparatus.

When analyzing the place cell metrics described above, only place cells which were active (met the place cell criteria) on a given condition contributed to that condition. If a place cell was not active on a given condition, its data was not included for that condition. For example, if a place cell was only active on 25° uphill, the metrics of its activity on 25° uphill were used, while the metrics for the other five conditions were not included in the calculation of those five condition's averages.

Place cell sequence plots

In order to visualise the activity of all the recorded place cells during a condition, sequence plots were created using firing rate maps. Sequence plots show the activity of many place cells by collapsing the short axis of the apparatus by averaging the firing rates of each short axis column along the long axis. Due to the narrow width of the shuttle box, there tended to be little deviation in place field width across the short axis. This transformation results in a one-dimensional (1D) vector of 2.5 cm^2 bins for the long axis of the apparatus. For our sequence plots, each row is a 1D vector of one place cell. Place cells can then be ordered based on the location of their place field, as determined by the bin with the peak firing rate. Place cell activity for any condition, say 15°, may then be arranged based on their field location in the apparatus in the 0° condition. This methods allows for the visualization of how much place cell activity changes when the apparatus is tilted from 0° to 15°. For visual clarity the firing rates of each place cell were normalised to be between 0 (minimum firing rate) and 1 (max firing rate) for a consistent z-axis. Firing rates for uphill plots and downhill plots were normalised separately.

Spatial activity correlations

While the place cell metrics described above capture how all active place cells were responding to tilt, we were also interested in how individual place cells were changing their activity due to changes in tilt. To test this, we utilized the occupancy maps for each place cell for each tilt condition and determined which bins were occupied on all three tilt conditions within a slope direction. Then, for each tilt condition the firing rate in each of the common-occupied bins were turned into a 1D vector and correlated between each pair of tilt conditions. There had to be a minimum of three common-occupied bins with non-zero firing rates to avoid spurious correlation values. In order to determine the importance of spatial

location, bin firing rates were randomly shuffled then correlated 10,000 times. The average correlation values from these 10,000 iterations were then compared to the actual correlation values.

Remapping

Remapping analyses were carried out by comparing how place cell's changed their activity within or between tilt conditions while keeping slope direction (uphill/downhill), and thus running direction, constant. Only place cells that met the place cell criteria for one or both of the two conditions being compared were deemed "active" and underwent more granular remapping analysis. Remapping analysis was conducted on the change in activity from the shallower tilt angle to the steeper tilt angle. Place cells which were not active on the two conditions being compared were deemed "inactive". Several different types of remapping were considered. Cells could "turn on" or "turn off" if they met the place cell criteria for one epoch but not the other (one type of complex remapping). For place cells which did meet the place cell criteria for both conditions in question, we determined if these cells field-remapped (the second type of complex remapping), rate remapped, or remained stable. First we tested if a place cell field-remapped by comparing the location of the bin with the maximum firing rate using the 1D place field maps of the two cells for both conditions. If their maximum firing rate bins differed by 20 cm, or ~20% of the running area, the place cell "field-remapped" in that its field location shifted from one epoch to the other. If the place cell did not field-remap, it was then determined whether its firing activity differed significantly between the two conditions. The firing rates of each trial for one condition were tested against the trial firing rates of the other condition with a Wilcoxon rank sum test. If the firing rates significantly differed ($P < 0.05$) then the place cell was considered to have "rate remapped" between the two conditions. Finally, if the activity of the place cell did not meet any of these remapping criteria between a pair of conditions it was considered to be "stable".

Further remapping analysis was carried out on place cells divided into "bottom" and "top" place cells depending on where their maximum firing rate was located in the maze in the 0° condition, with "top" being that half of the maze that was raised highest in the tilt conditions.

Phase precession Analysis

To quantify how the timing of spikes relative to the underlying theta rhythm changed as animals moved through each place field, an analysis of phase precession (O'Keefe & Recce, 1993; Skaggs et al., 1996) was conducted. For phase estimation, the CA1 LFP was bandpass filtered between 7 and 9 Hz and the Hilbert transform was applied. The phase reference was always to the LFP in the CA1 pyramidal cell layer theta, and 0° corresponds to the trough in the negative portion of the filtered LFP. Place field position was determined automatically by dividing the shuttlebox into 4 x 20 pixels and selecting clusters of pixels that were in the region of the apparatus that excluded reward areas and where cells fired at above average firing rate and had at least two neighbors that also did so. Place fields were detected separately for each of the slope conditions and where more than one place field was found for a cell in a condition, data from the largest field was analyzed. All place field determination and data analysis were from data obtained as the animal ran in the same direction, either up the slope or on the flat.

For all spikes that occurred with a place field, spike phase was determined by matching animal position in the field to the instantaneous phase of the 7-9 Hz theta rhythm. The relationship between phase and position in each place field was measured using procedures described previously (Kempter, Leibold, Buzsaki, Diba, & Schmidt, 2012). Briefly, his involves using circular-linear regression procedures to provide a robust estimate of the slope and phase offset of the regression line, and a correlation coefficient for circular–

linear data that is a natural analogue of Pearson's product-moment correlation coefficient for linear–linear data. This procedure gets around the potential problems associated with using linear-linear correlation on circular data. The fits were constrained to have a slope of no more than ± 2 theta cycles per place field transverse. Previous studies indicate that phase precession occurs with a negative slope (O'Keefe & Recce, 1993). Phase precession analysis was conducted by combining spiking data from all passes through the place field for all cells that had a total of at least 50 spikes within the place field in the condition of interest and where the magnitude of the amplitude envelope of the filtered EEG, as derived from the Hilbert transform and tested for each spike at the time of firing, was above the mean. These constraints removed noise in the data potentially produced by low firing-rate cells or spikes that occurred when EEG amplitude was low and therefore phase determination might be problematic. Analysis of firing, phase-position slope and correlation data was conducted using a between subjects ANOVA on individual cell data. The phase offset data, which corresponded to the theta phase at which spiking occurred as the animal entered the field was compared across conditions using circular statistics, including the Watson-Williams test for comparison of circular data (Zar, 1999).

Histology

After completion of behavioral testing the placement of the tetrodes were confirmed by creating a lesion at the tip of each tetrode by passing 2 mA of current for one second on two wires of each tetrode while the rat was deeply anesthetized with isoflurane. Rats were subsequently overdosed on isoflurane in a large bell jar and perfused transcardially with 120 ml of 0.9% saline followed by 120 ml of 10% formalin in saline. Brains were removed and placed in 30% sucrose solution until they sunk. Brains were then frozen and sliced with a microtome (Lecia Biosystems, LLC) to 60 μm thick coronal sections. Sections were mounted and stained with thionine acetate (Santa Cruz Biotechnology, Inc.) and tetrode placement was

confirmed with a lower power (1.5x) digital microscope (Lecia Biosystems, LLC) and tetrode movement logs.

Results

Rodent behavior and place cell properties

We recorded single units from the dorsal CA1 subregion of well-trained rats as they shuttled back and forth in a shuttle box which could be laid flat (0°) or tilted to 15° or 25° to manipulate tilt (Fig. 1a). Behavioral and neurophysiological data were only analyzed in the running region of interest with the rewarded endzone regions excluded (Fig. 1b). Data was collected over six consecutive days, with counterbalancing for tilt condition presentation order and which side was elevated (Fig. 1c). The rats completed an average of 18.8 (Standard Error of Mean; SEM ± 0.17) successful trials (i.e., did not turn around, took less than 7 seconds) for each tilt angle-slope direction (tilt angles: 0°, 15°, and 25°; slope directions: uphill and downhill). Rat's running speeds were significantly influenced by tilt ($F(2, 74) = 19.88$, $P < 0.0001$), slope direction ($F(1, 37) = 9.897$, $P = 0.0033$), and their interaction ($F(2, 74) = 10.33$, $P < 0.0001$; Fig. 1d). On average, rats slowed down with an increasing tilt angle, running an average speed of 33.1 cm/s (SEM ± 0.9) on 0°, 32.1 ± 0.8 cm/s on 15°, and 28.3 ± 0.7 cm/s for 25°. Surprisingly, rats were significantly faster on 15° (33.4 ± 1.1 cm/s) and 25° (30.0 ± 1.0 cm/s) uphill than on 15° (31.5 ± 1.2 cm/s; (Tukey's; $q(74) = 5.363$, $P = 0.004$) and 25° (26.6 ± 1.0 cm/s; Tukey's; $q(74) = 6.98$, $P < 0.001$) downhill, respectively. Running speeds on 0° "uphill" (32.7 ± 1.2 cm/s) and "downhill" (33.4 ± 1.2 cm/s) did not differ significantly (Tukey's; $q(74) = 1.58$, $P = 0.874$). Anecdotally, rats tended to employ a fast hopping-like gait when travelling uphill and a more cautious walk for downhill runs. Tilt also significantly affected ($F(2, 74) = 13.51$, $P < 0.001$) the way in which rats travelled in the

shuttle box; as the tilt angle increased, rats ran more irregular routes as observed by the total number of 2.5cm^2 bins they occupied in a given condition (slope direction: $F(1, 37) = 0.8214$, $P = 0.3706$); interaction: $F(2, 74) = 2.427$, $P = 0.0953$; Fig. 1e). Rats utilized significantly more area to run on 25° compared to 0° (Tukey's; $P < 0.0001$) and 15° ($P = 0.0001$). In conjunction with previous physiological studies on rats running inclined and declined treadmills (Armstrong et al., 1983; Brooks & White, 1978; Chavanelle et al., 2014), the reduction in running speed and more irregular paths likely indicate the difficulty of travelling on sloping terrain.

The effects of tilt on place cell encoding

A total of 225 putative single units were recorded across all recording sessions from the seven rats. Of those cells, 99 met our strict place cell criteria for inclusion in subsequent analyses with an average of 14.1 ± 4.0 place cells (PCs) recorded per rat (Rat 1, 25; Rat 2, 4; Rat 3, 1; Rat 4, 6; Rat 5, 18; Rat 6, 17; Rat 7, 28). We were interested in whether there were systematic changes to standard measures of place cell activity as our apparatus was tilted. Overall, tilt and slope direction appeared to have little effect on most measures of place cell activity (Table 1). Two-way ANOVAs with tilt (0°, 15°, 25°) and slope direction (uphill, downhill) as factors revealed no significant difference ($P > 0.05$) for either factor or their interaction when comparing mean firing rates, peak firing rates, spatial information, or spatial coherence. Tilt angle did have a small but significant effect ($F(2, 206) = 3.056$, $P = 0.0492$) on the sparsity of place cell firing (slope; ($F(1, 206) = 0.414$, $P = 0.5204$) interaction; ($F(2, 206) = 0.565$, $P = 0.5692$)). Tukey's test for multiple comparisons revealed a significant difference between the average sparsity of place cell activity on 0° compared to 25° (Tukey (206) = 3.401, $P = 0.0448$), and no differences between 0° to 15° and 15° to 25° ($P > 0.05$). Due to the differences in the number of bins rats occupied across conditions, we measured place field sizes as a percentage of occupied area covered by the place field (place field size /

477 total bins occupied). Neither tilt nor slope direction affected the number of fields place cells
478 had, the total coverage of all place fields, or the size or aspect ratio of a cell's main place
479 field ($P > 0.05$). Furthermore, infield firing rates and outfield firing rates did not differ across
480 tilt or slope conditions ($P > 0.05$).

481

482 *Place cells remap in response to tilt*

483 Previous studies have demonstrated that place cells will alter their activity, or
484 "remap" in response to manipulations to an environment, such as changes to the shape of
485 environments or visual cue locations (Muller & Kubie, 1987). We were initially interested in
486 how place cell activity was remapping in response to changes in tilt. A diverse range of
487 remapping responses to the tilt manipulation were observed from place cells recorded in
488 different animals (Figure 2). Most place cells met the place cell criteria for either one (38%
489 Fig. 3a; e.g. Fig. 2a), two (29%; e.g. Fig. 2b), or three of the slope x direction conditions
490 (20%; e.g. Fig. 2c,d,f), with very few meeting the criteria for four (7%), five (2%), or all six
491 (3%; e.g. Fig. 2e). On average, cells met the place cell criteria for 2.1 conditions (SEM ±
492 0.12). There was no significant difference in the number of place cells active for a given tilt
493 angle (0° = 78, 15° = 70, 25° = 74; X^2 (2) = 0.27, P = 0.867), however there were
494 significantly more place cells active on downhill conditions (n = 125) versus uphill
495 conditions (n = 87; X^2 (1) = 6.81, P = 0.009; Fig 3b). During both uphill and downhill
496 conditions, most place cells were active on one of the three tilt conditions, with fewer active
497 on two or three condition (Fig 3c). The number of tilt conditions place cells were active for
498 did not differ significantly between uphill and downhill conditions (X^2 (2) = 2.12, P = 0.333).
499 Most place cells (71%) exhibited directional selectivity (Fig. 2a-d,f) and only met the place
500 cell criteria for one slope direction (Fig. 3d). In contrast, 29% of place cells showed

bidirectional activity and were active on both uphill and downhill runs (Fig. 2e). There were no significant differences in the number of unidirectional versus bidirectional place cells across the tilt conditions (X^2 (2) = 2.22, P = 0.329). Taken together, place cells tend to be unidirectional and selectively active on specific tilt-slope direction conditions.

Place cell remapping across conditions

We wanted to further quantify the types of remapping cells were undergoing as the tilt of the environment was manipulated. We analysed whether or not place cells remapped between conditions and if they did remap, what type of remapping they underwent. For each place cell, we asked how it was changing its activity between each pair of tilt conditions while keeping slope direction constant (Fig 3e). A Chi-squared test determined there were no differences in the number of place cells undergoing rate or field remapping, turning on or off, or remaining stable across the condition pairs (X^2 (25) = 29.29, P = 0.252). Because there were no differences, we will present the average percentage of place cells across the six condition pairs which underwent each type of remapping. On average, 51% ± 3% of recorded place cells were inactive between a given pair of tilt conditions. If a place cell was active on two conditions, complex remapping was the most common form of activity change with place cells either turning on (16% ± 1%) or shutting off between conditions (14% ± 1%). Field remapping was quite rare, with an average of just 1.3% ± 0.4% cells remaining active on two conditions but with distinct place field locations. Rate remapping, where place cells have a stable field location but significantly alter their firing rate between two conditions, was more common with an average of 7% ± 1% place cells. Lastly, an average of 10% ± 2% of place cells had stable activity between two conditions. These results further indicate that the degree of change between tilt angles does not have an effect on the magnitude or type of place cell remapping. Rather, any change to the tilt of an environment results in place cell ensembles undergoing consistent but substantial partial-complex remapping.

Place cell sequence plots

To visualize the place cell remapping that was occurring across tilt conditions we generated a series of sequence plots. Here, all 99 place cells that were active for at least one slope direction-tilt condition (tilt: 0°, 15°, and 25°; slope direction: uphill and downhill) were included in the plots. For each place cell, the firing rates across the apparatus in all conditions is displayed as heat maps and for each condition. Place cells are ordered according to their place field position in the apparatus using one tilt x slope direction condition as a baseline and plotting the other conditions relative to this baseline.

Sequence plots were created and ordered according to the place field sequence order for all three tilt conditions (0°, 15°, 25°), separately for each slope direction (uphill or downhill) (Fig. 4). A grey outline of the sequence plot and asterisk in the condition title indicates which condition is being used to organize the place cells by their field location in that condition. Changes in the tilt of the apparatus results in a wide range of remapping activity with some place cells turning on or off while others remain active across tilt conditions with changes to their field location or firing rate. Overall, place field sequences tend to hold their ordered sequence across the different tilts, suggesting that at least some place cell fields are stable on different tilt angles. We also ordered place cells from one slope direction, and thus running direction, to the other which showed a near total breakdown in place field sequence across the environment (data not shown). Thus, tilting a fixed environment causes substantial, partial-complex remapping of place cell populations for both uphill and downhill trajectories.

Place cell activity across tilt and slope conditions

In order to quantify the effects of tilt shown in the sequence plots, a spatial correlation analysis was utilised to test how individual place cells were being affected by changes in tilt

and slope direction. We hypothesized that place cells may use tilt angle as a way to discriminate between experiences. If this is so, conditions where the tilt angle is more similar (15° to 25°; 10° difference) should be more correlated to each other compared to conditions where the tilt angle is more different (0° to 25°; 25° difference). For each place cell we computed a correlation comparing the firing rates of each bin commonly-occupied between the two conditions, for every tilt-slope direction pair. We then aggregated the correlation values from every place cell for each pair of conditions (Figure 5). A two-way ANOVA showed no significant effect for slope direction ($F(1, 285) = 3.51$, $P = 0.0620$), the difference in tilt angle between tilt pairs ($F(2, 285) = 0.8864$, $P = 0.4133$), or their interaction ($F(2, 285) = 0.0500$, $P = 0.9516$). We further tested these data against correlation values generated from randomly shuffling firing rate bin locations for each condition pair. For all six pairs of conditions, the actual correlation values were significantly greater from those that would be generated by chance if spatial specificity was irrelevant (Wilcoxon rank sum test; $P < 0.001$). These data suggest that overall dCA1 place cells treat each tilt condition as a unique environment and form distinct maps for each condition, however, these maps are not completely unrelated.

Place cell remapping between and within conditions

In order to confirm that the place cell activity changes apparent across the different tilt conditions were due to changes in tilt and not simply due to changes in place cell activity over time, we compared within-tilt condition changes with those observed between different tilt conditions across similar time windows. Place cell activity was compared within the second and third tilt conditions for each recording session by analyzing how place cells remapped from the first 10 trials to the second 10 trials. To test the effect of changing tilt, the latter 10 trials from the first tilt condition were compared to the first 10 of the second condition and the latter 10 of the second to the first 10 of the third. When place fields were

575 characterized by the type of remapping observed across these two comparisons, it was
576 apparent that remapping was quite different in the tilt-change comparison compared to the
577 within-condition situation (X^2 (4) = 23.5, P < 0.001, Chi-squared test; Table 3). We further
578 combined all forms of remapping into one category to test against stable place cells. Place
579 cells were significantly more likely to remain stable within a tilt condition compared to
580 between tilt conditions (X^2 (1) = 16.6, P < 0.001). Together, these data indicate that the
581 change in place cell response across tilt angles cannot simply be explained as instability over
582 time.

583 *Elevation change has no effect on remapping*

584 We next set out to test whether or not the tilt-associated remapping we were observing
585 was related to the tilt per se or to the vertical transition in space that occurred across most of
586 the apparatus as it was shifted from the flat to tilted condition. We hypothesized that if place
587 cells were encoding the elevation of the apparatus it would be expected that the further a
588 place field moved through 3D space (primarily vertically) the more likely it would be for a
589 place cell to remap. To these ends we divided the apparatus up into two halves with the
590 knowledge that overall one half (high) was shifted through space to a greater extent than the
591 other half (low) when the apparatus was shifted from the flat to the sloped condition (see Fig.
592 1a). We first considered all place cells which met the place cell criteria for the 0° tilt
593 condition in either slope direction. The place cell's field location in the bottom or top of the
594 apparatus was determined from the bin of the 1D place field map that had the maximal firing
595 rate. For those place cells that were active in the 0° condition we then asked how changes in
596 elevation altered their activity. We discovered that place cells with fields on the low half of
597 the apparatus were just as likely to remap (turn on/off/field/rate) or remain stable as place
598 cells with fields on the high half of the apparatus (X^2 (1) = 1.635, P = 0.201; Table 2).
599 Differentiating between complex remapping (turn on/off, field remap), rate remapping, and

600 stable place cells also shows no significant effect for a field's vertical transition (X^2 (2) =
601 2.89, P = 0.236). This analysis was also repeated using a place cell's center of mass location
602 rather than maximal firing rate location to determine the top/bottom categorizing factor, with
603 no difference in results (P > 0.05). Thus, remapping is likely driven directly by the change in
604 the slope, with cells remapping to encode a particular whole-tilt 'context', rather than being
605 an effect of the vertical transition of part of the apparatus.

606 *Phase precession analysis*

607 Data for phase precession analysis was gathered from 78 cells that met the sampling criteria
608 at zero degrees of tilt, 79 cells at 15 degrees and 92 cells at 25 degrees (Figure 6a). All
609 analysis was conducted for travel up the tilted surface or for the equivalent direction on the
610 flat. A quantification of phase precession characteristics was provided through the circular-
611 linear correlation procedure, which indicated no difference between tilt conditions in terms of
612 the proportion of cells that generated statistically significant (P <0.05) circular-linear fits (X^2
613 = 4.91, P = 0.09). Overall, there was also no difference in the circular linear correlation
614 coefficient calculated for the three different slope conditions (F (2,245) = 1.359, P = 0.259.
615 However, a comparison of the best fit line through the data indicated some differences
616 between tilt conditions. For all groups, the initial firing as the animal entered the place field
617 tended to occur on the rising phase of the theta cycle as we recorded it at the CA1 pyramidal
618 cell layer, equivalent to firing occurring just after the peak of theta at the fissure as described
619 previously (Skaggs et al., 1996). There was, however, a significant shift towards an earlier
620 firing phase as the tilt of the apparatus increased (Rayleigh's F = 7.25, P < 0.001; Fig. 6b). A
621 comparison of the slope of the best-fit to the data measuring the precession across the theta
622 cycle indicated that slope decreased to become less-negative as the tilt of the apparatus
623 increased (F (2,246) = 3.64, P = 0.028; Fig 6c). These changes in phase precession did not
624 appear to be artifacts of other changes in cell firing or animal movement as no significant

between-tilt differences were observed in mean firing rate within the field, place field width, place field position, theta frequency, theta amplitude or animal speed within the field (all $P > 0.1$).

Discussion

To understand how a change in the slope of a traversed surface influenced the hippocampal representation of space, we analyzed the activity of dCA1 place cells as rats shuttled back and forth in a high-sided box tilted at 0°, 15°, and 25° angles. Our data indicated that place cells had no loss of spatial specificity on tilted environments as demonstrated by standard place cell metrics. Nevertheless, place cells are sensitive to changes to the tilt angle of an environment. We showed that any change to the tilt of the shuttle box led to substantial partial remapping of place fields. However, the magnitude of the difference in tilt angle between conditions did not reflect the degree of remapping observed. In addition, the probability of a place cell remapping was not affected by how far the animal moved in the vertical dimension of space which supports the proposal that rodent place cells encode space anisotropically (Jeffery et al., 2013).

A well-studied characteristic of hippocampal place cells is their ability to "remap" their activity in response to changes to the environment (Colgin, Moser, & Moser, 2008; Leutgeb et al., 2005; Muller & Kubie, 1987). Most commonly, changes to the shape or size of the environment or the locations of prominent cues can result in alterations in place cell firing, including changes in firing rate or changes in the location of the place field. Place cell remapping to changes in the tilt of an environment have, however, seldom been investigated despite previous studies showing that place cells respond to changes in vestibular information (Russell et al., 2003; Stackman et al., 2002) and can use slope as an orienting cue (Jeffery et al., 2006). Our data showed that a high proportion of place cells remapped as the tilt of the

649 shuttle box was manipulated. As a result, many cells were only responsive to one or two of
650 the tilt slope-direction conditions; demonstrating the sensitivity of place cells to slope terrain.
651 However, place cell encoding does not seem to be coupled to changes in slope angles as
652 irrespective of whether the shuttle box slope was altered by 10° (15° to 25°) or 25° (0° to
653 25°), similar levels and types of remapping were observed. These data indicate that the
654 hippocampus is encoding each tilt condition as a discrete context with terrain slope as a
655 differentiating cue.

656 A subset of place cells did remain active, with a stable place field location and firing
657 rate, on more than one tilt condition. These place cells may aid in associating together these
658 experiences (Eichenbaum, 2004; Leutgeb, Leutgeb, Treves, Moser, & Moser, 2004;
659 McKenzie, Frank, Kinsky, Porter, Rivière, et al., 2014). Stable place cells, especially those
660 active on two tilt conditions within a slope direction, may accomplish this associative
661 function by having a broader terrain slope tuning curve than other cells. An alternative, and
662 not mutually exclusive, explanation is that subsets of place cells are utilizing different
663 reference frames for their spatial specificity (Gothard et al., 1996; Knierim & Hamilton,
664 2011; Wiener, Korshunov, Garcia, & Berthoz, 1995; Zinyuk, Kubik, Kaminsky, Fenton, &
665 Bures, 2000). These stable place cells, especially those active on all three tilt conditions
666 within a slope direction, may be driven by egocentric, path integration information which is
667 resilient to changes in terrain slope and remain stable when terrain slope is altered.

668 To our knowledge only one previous study has investigated how place cells respond
669 to tilting an environment (Knierim & McNaughton, 2001). Knierim and McNaughton (2001)
670 showed that when part of a square track was tilted from 0° to 45°, partial remapping
671 occurred. No consistent change in other metrics, such as peak firing rate, was found. In this
672 previous study, however, the track had no side walls and was located such that animals had a
673 clear view of distal visual cues in the recording room. For this reason, we cannot be sure if

674 the remapping observed in this previous study was a result of the tilt itself, or a response to
675 the apparent shift of the distal cue locations that would have accompanied the track
676 manipulation. In contrast, in the present study we have endeavored to minimize the influence
677 of the tilt manipulation on distal cues by depriving the animal of any visual clues that might
678 have become associated with a tilt condition. Our remapping findings are therefore consistent
679 with those previously reported by Knierim and McNaughton (2001), but further constrain
680 interpretations of the effect tilt has on place cell encoding.

681 A recent study by Hayman et al. (2015) found that medial entorhinal (MEC) grid cell
682 activity was disrupted between flat and tilted (40°) terrain. Primarily, grid cells had decreased
683 spatial coherence and lower symmetry with larger and more numerous fields. We had
684 hypothesized that hippocampal place cell activity may also be disrupted on tilted terrain in a
685 similar fashion because experimental and computational evidence has demonstrated that the
686 MEC and grid cells are an important source of information for hippocampal place cells
687 (McNaughton, Battaglia, Jensen, Moser, & Moser, 2006; Ormond & McNaughton, 2015; F.
688 Savelli & Knierim, 2010). We did not observe any significant changes in place cell activity
689 across our three tilt conditions. It may be possible that place cells activity could be disrupted
690 on very steep slopes, such as the one used by Hayman et al. (2015), and that 25° is not
691 sufficient to disrupt encoding. However, our findings are in line with recent experimental
692 (Miao et al., 2015; Rueckemann et al., 2016) and computational models (Azizi, Schieferstein,
693 & Cheng, 2014) which show that hippocampal place cell activity can be resilient to
694 disruptions to the MEC. Hippocampal units may rather rely on other, non-MEC spatial
695 inputs, such as head direction (Stackman & Taube, 1998; Taube, Muller, & Ranck, 1990) and
696 border cells (Lever, Burton, Jeewajee, O'Keefe, & Burgess, 2009), to generate the spatial
697 selectivity of place cells (Bush, Barry, & Burgess, 2014).

Since our tilt procedure involved pivoting the shuttle box around one of its ends (Fig 1), the shift in the vertical position of any location in the apparatus during a tilt manipulation depended on the distance from that location to the pivot point. We used this difference to allow for an investigation of the remapping of place fields in the half of the box close to the pivot (small vertical shift) compared to those in the half distal to the pivot (large vertical shift). If the hippocampal representation of space in rats were volumetric and isotropic, as suggested by the discovery of 3D, spherical place fields in freely flying bats (Yartsev & Ulanovsky, 2013), one might anticipate that place cells with fields in the half of the box that had the greatest vertical movement through space would have a higher likelihood of remapping as the animals were shifted out of, or into, the vertical confines of particular place cell fields. Our analysis indicated, however, that the propensity for a place cell to remap was not affected by the half in which the cell's field was located, suggesting that in surface-travelling-mammals, such as rats, representations of space both by hippocampal place cells (Hayman et al., 2011) and entorhinal grid cells (Hayman, Casali, Wilson, & Jeffery, 2015) are planar and anisotropic (Jeffery et al., 2013).

An analysis of phase precession processes indicated that there were systematic changes to the way that spike firing related to the underlying local theta rhythm as tilt changed. In particular, firing began earlier in the theta cycle when the animal was entering a place field on a tilted surface. Furthermore, the amount of phase precession decreased as the slope increased. These effects could not be explained as artifacts of changes in variables such as theta frequency or amplitude, or animal running speed. It is unclear what function, if any, this change represents, however, it is possible that it might alter how the hippocampus 'interpreted' the environment. Previous studies suggest that phase precession provides a constant 'look-ahead' function that allows for the planning of future trajectories (Skaggs et al 1996; Wikenheiser and Redish, 2015). At any particular moment, a decrease in the slope of

723 phase precession would compress the components of these trajectory predictions into a
724 narrower time window. A potential consequence of this change is the enhancement of
725 plasticity between cells representing distal regions through the opening of a temporal window
726 for synapse potentiation that might not exist when spikes are temporally more distant (Dan &
727 Poo, 2004). One result of this effect might be an expansion of place field size as cells gain
728 greater influence over the firing of their distal (in terms of place field) neighbors. We did not
729 see evidence of this expansion, although it has previously been observed to co-occur with
730 reduced phase precession slope (Shen, Barnes, Mcnaughton, Skaggs, & Weaver, 1997;
731 Terrazas et al., 2005). It is possible, however, that such an expansion effect might only occur
732 during the initial exposure to an environment, and then influence subsequent responses to
733 other similar environments, such that in our well-trained animals, the expression of this effect
734 occurred on all slopes. This could be tested in future studies by only exposing animals to one
735 slope condition and then examining the consequences on place field size. If an initial
736 exposure to a novel slope does produce an expansion of place field size then this might lead
737 to a perception that sloped surfaces extend further than they actually do (Proffitt, Stefanucci,
738 Banton, & Epstein, 2003; Stefanucci, Proffitt, Banton, & Epstein, 2005; Witt, Proffitt, &
739 Epstein, 2004). It is tempting to speculate that this might underlie a neural instantiation of
740 Naismith's rule that slopes will take longer to traverse relative to the same distance on flat
741 ground, although further studies will be required to determine whether this is so.

742 Overall, we have observed that a subset of hippocampal place cells are sensitive to
743 changes to terrain slope. The encoding of terrain slope is a vital element of efficient
744 navigation allowing an organism to avoid the time and energy costs associated with traveling
745 uphill (Armstrong et al., 1983; Brooks & White, 1978; Chavanelle et al., 2014; Hoogkamer et
746 al., 2014; Margaria et al., 1963; Minetti et al., 2002). Additionally, our findings contribute to
747 the wider field of cost-benefit analysis in the context of spatial navigation. Growing evidence

748 has shown that place cells respond to the value of an experience (Allen, Rawlins, Bannerman,
749 & Csicsvari, 2012; Ambrose, Pfeiffer, Correspondence, & Foster, 2016; Cheyne, 2014;
750 Gauthier & Tank, 2017; McKenzie, Frank, Kinsky, Porter, Rivière, et al., 2014). Our data
751 show that there are more place cells active on downhill runs versus uphill runs on the tilt
752 conditions. This is unlikely to be due to speed differences, which if anything, would produce
753 the opposite effect, with the slower downhill movement usually associated with reduced
754 firing. Rather, this may indicate that the downhill route may have a greater relative value
755 (benefit minus effort cost) and so has a larger ensemble of place cells representing it. Indeed,
756 previous studies have shown that place cells over-represent goal locations (Hollup et al.,
757 2001; Cheyne, 2014) and preferred routes (Mamad et al., 2017).

758 During decision making, possible behaviors as well as their remembered values may
759 be sent to downstream structures through the reactivation of place cell ensembles via sharp-
760 wave ripple replay events (Jadhav, Kemere, German, & Frank, 2012; Pfeiffer & Foster, 2013;
761 Singer, Carr, Karlsson, & Frank, 2013) or theta sequences (Johnson & Redish, 2007;
762 Wikenheiser & Redish, 2015). Our findings that place cells can encode terrain slope may aid
763 in providing downstream cortical structures, such as the anterior cingulate cortex (Remondes
764 & Wilson, 2013, 2015), not only with previous and possible routes through an environment
765 but with effort information associated with those routes (Cowen, Davis, & Nitz, 2012;
766 Hillman & Bilkey, 2010, 2012). As a result, prefrontal regions may selectively retrieve and
767 reactivate the highest value hippocampal representations (Ito, Zhang, Witter, Moser, &
768 Moser, 2015; Navawongse & Eichenbaum, 2013; Preston & Eichenbaum, 2013), resulting in
769 the further differentiation of hippocampal ensembles based on value.

770

771

Figure legends

Figure 1: Experimental setup and behavioral results. a) Pictures of the experimental apparatus at the three tilt conditions with the location of the camera marked. b) Schematic of the apparatus, the boundaries (dashed line) of the running region of interest and two endzones. The solid black tracing is the tracking data from one recording session showing the rat's running pattern. c) Experimental sequence. Rats were run for six consecutive days with

tilt condition presentation order counterbalanced across days. d) Average running speed of the rats across all tilt-slope direction conditions. Rat's speed slowed with increasing tilt angle and was slowest for downhill runs. Bars sharing the same letter are significantly different from one another. (a) Tukey's, $P = 0.004$ between uphill 15° and downhill 15°; (b) Tukey's, $P < 0.001$ between uphill 25° and downhill 25°. e) The amount of space rats utilized while shuttling. Rat's tended to take more irregular routes on tilted conditions. Bars sharing the same letter are significantly different from one another. (a) Tukey's, $P < 0.0001$ between 0° and 15°; (b) Tukey's, $P < 0.0001$ between 0° and 25°.

Figure 2: Six example place cell firing rate maps (a-f), with firing of each cell illustrated across all six conditions. Every subplot shows the experimental apparatus as a series of 2.5 cm2 bins with the x and y axes corresponding to position in the shuttle box. The z-axis is the firing rate of the cell in spikes per second (Hz) for each bin where warmer colors indicate a higher firing rate. For each place cell, the firing rate color scale across the three conditions is determined by the highest peak firing rate of the six tilt conditions. The left column of a plot shows Downhill runs while the right column shows Uphill runs. Each row of a plot corresponds to one of the three tilt conditions; top, 0°; middle, 15°; bottom, 25°. Note that several cells fired specifically for one or two tilt conditions (e.g. a and b).

Figure 3: Place cell encoding of tilt conditions. a) The number of tilt-slope direction conditions place cells were active for. b) The percent of place cells active for each tilt-slope direction condition. c-d) The number of tilt conditions (c) or slope direction conditions (d) place cells were active for. e) Types of remapping observed between pairs of tilt conditions within a slope direction comparing shallower angles to steeper angles.

Figure 4: Place cell sequence plots. Thus, the x-axis represents the longitudinal extent of the apparatus and each row of the y-axis is a place cell. Place cells are ordered based on their field location of one of the three tilt conditions (0°, 15°, and 25°; from left to right) which served as the baseline. The baseline condition is indicated by a grey border and an asterisk in the title. The z-axis is a cell's normalized firing rate; warmer colors represent a higher firing rate. Changes to the tilt have a substantial complex remapping effect on place cells as evidenced by the number of cells that turn on or off with a change in condition. Cells that are active for multiple tilt conditions generally have a stable place field location in the maze as indicated by the preserved place field location sequence across changes in tilt.

Figure 5: Place cell activity correlations across tilt-slope direction conditions. All plots show a histogram of correlations values of place cell activity between pairs of conditions. The dotted line is the average correlation value from shuffling the location of firing rate bins. No significant differences were found in the difference in tilt angle to the degree of place cell activity difference on uphill or downhill runs.

Figure 6: Phase precession. a) Examples of the phase precession of place cell spiking against theta activity as the animal traverses the place field from left to right. Zero degrees 0° corresponds to the trough in the negative portion of the filtered LFP recorded at the CA1 cell layer. Data points are reproduced twice over two theta cycles. The left plot is recorded from an animal moving on a flat surface while the middle two are tilted at 15° and the rightmost, 25°. b) Place cell firing phase, with reference to the underlying local theta as the animal enters the place field, is systematically shifting to earlier in the cycle as the apparatus is tilted. Data are mean angle and circular sem. c) Phase precession slope decreases as the apparatus is tilted. The data are degrees per cycle.

842

843

844

845

846

847

848

849

850

851

852

853

854

855

856

857 **References**

858 Allen, K., Rawlins, J. N. P., Bannerman, D. M., & Csicsvari, J. (2012). Hippocampal place
859 cells can encode multiple trial-dependent features through rate remapping. *Journal of*
860 *Neuroscience*, *32*(42), 14752–14766.

861 Ambrose, R. E., Pfeiffer, B. E., Correspondence, D. J. F., & Foster, D. J. (2016). Reverse

862 replay of hippocampal place cells is uniquely modulated by changing reward. *Neuron*,
863 *91*, 1–13.

864 Armstrong, R. B., Laughlin, M. H., Rome, L., & Taylor, C. R. (1983). Metabolism of rats
865 running up and down an incline. *Journal of Applied Physiology*, *55*, 518–521.

866 Azizi, A. H., Schieferstein, N., & Cheng, S. (2014). The transformation from grid cells to
867 place cells is robust to noise in the grid pattern. *Hippocampus*, *24*, 912–919.

868 Bilkey, D. K., & Muir, G. M. (1999). A low cost, high precision subminiature microdrive for
869 extracellular unit recording in behaving animals. *Journal of Neuroscience Methods*,
870 *92*(1–2), 87–90.

871 Brooks, G. A., & White, T. P. (1978). Determination of metabolic and heart rate responses of
872 rats to treadmill exercise. *Journal of Applied Physiology*, *45*, 1009.

873 Bush, D., Barry, C., & Burgess, N. (2014). What do grid cells contribute to place cell firing?
874 *Trends in Neurosciences*, *37*(3), 136–145.

875 Chavanelle, V., Sirvent, P., Ennequin, G., Caillaud, K., Montaurier, C., Morio, B., …
876 Richard, R. (2014). Comparison of oxygen consumption in rats during uphill
877 (concentric) and downhill (eccentric) treadmill exercise tests. *Journal of Sports Science*
878 *and Medicine*, *13*, 689–694.

879 Cheyne, K. R. (2014). *Hippocampal Place Cells Dynamically Encode Value of Available.*
880 *Goals During Spatial Navigation* (Unpublished doctoral dissertation). University of
881 Otago, Dunedin, New Zealand.

882 Colgin, L. L., Moser, E. I., & Moser, M. B. (2008). Understanding memory through
883 hippocampal remapping. *Trends in Neurosciences*, *31*(9), 469–477.

884 Cowen, S. L., Davis, G. A., & Nitz, D. A. (2012). Anterior cingulate neurons in the rat map

885 anticipated effort and reward to their associated action sequences. *Journal of*
886 *Neurophysiology*, *107*, 2393–2407.

887 Dan, Y., & Poo, M. M. (2004). Spike timing-dependent plasticity of neural circuits. *Neuron*,
888 *44*, 23–30.

889 Di Fiore, A., & Suarez, S. A. (2007). Route-based travel and shared routes in sympatric
890 spider and woolly monkeys: Cognitive and evolutionary implications. *Animal Cognition*,
891 *10*, 317–329.

892 Eichenbaum, H. (2004). Hippocampus: Cognitive processes and neural representations that
893 underlie declarative memory. *Neuron*, *44*, 109–120.

894 Finkelstein, A., Derdikman, D., Rubin, A., Foerster, J. N., Las, L., & Ulanovsky, N. (2014).
895 Three-dimensional head-direction coding in the bat brain. *Nature*, *517*(7533), 159–164.

896 Fyhn, M., Hafting, T., Treves, A., Moser, M.-B., & Moser, E. I. (2007). Hippocampal
897 remapping and grid realignment in entorhinal cortex. *Nature*, *446*(7132), 190–4.

898 Gauthier, J. L., & Tank, D. W. (2017). *Context-invariant encoding of reward location in a*
899 *distinct hippocampal population* (No. bioRxiv 207043).

900 Gothard, K. M., Skaggs, W. E., Moore, K. M., & McNaughton, B. L. (1996). Binding of
901 hippocampal CA1 neural activity to multiple reference frames in a landmark-based
902 navigation task. *The Journal of Neuroscience*, *16*(2), 823–835.

903 Hayman, R., Casali, G., Wilson, J. J., & Jeffery, K. J. (2015). Grid cells on steeply sloping
904 terrain: evidence for planar rather than volumetric encoding. *Frontiers in Psychology*,
905 *6*(925), 1–14.

906 Hayman, R., Verriotis, M. A, Jovalekic, A., Fenton, A. A, & Jeffery, K. J. (2011).
907 Anisotropic encoding of three-dimensional space by place cells and grid cells. *Nature*

908 *Neuroscience*, *14*(9), 1182–1188. 2

909 Hillman, K. L., & Bilkey, D. K. (2010). Neurons in the rat anterior cingulate cortex
910 dynamically encode cost-benefit in a spatial decision-making task. *The Journal of*
911 *Neuroscience*, *30*(22), 7705–7713.

912 Hillman, K. L., & Bilkey, D. K. (2012). Neural encoding of competitive effort in the anterior
913 cingulate cortex. *Nature Neuroscience*, *15*(9), 1290–1297.

914 Hollup, S. A., Molden, S., Donnet, J. G., Moser, M.-B., & Moser, E. (2001) Accumlation of
915 hippocampal place fields at the goal location in an annular watermaze task. *The Journal*
916 *of Neuroscience*, *21*(5), 1635-1644.

917 Hoogkamer, W., Taboga, P., & Kram, R. (2014). Applying the cost of generating force
918 hypothesis to uphill running. *PeerJ*, *2:e482*.

919 Ito, H. T., Zhang, S., Witter, M. P., Moser, E. I., & Moser, M. (2015). A prefrontal–thalamo–
920 hippocampal circuit forgoal-directed spatial navigation. *Nature*, *522*(7554), 50–55.

921 Jadhav, S. P., Kemere, C., German, P. W., & Frank, L. M. (2012). Awake hippocampal
922 sharp-wave ripples support spatial memory. *Science*, *336*(6087), 1454–8.

923 Jeffery, K. J., Anand, R. L., & Anderson, M. I. (2006). A role for terrain slope in orienting
924 hippocampal place fields. *Experimental Brain Research*, *169*, 218–225.

925 Jeffery, K. J., & Anderson, M. I. (2003). Dissociation of the geometric and contextual
926 influences on place cells. *Hippocampus*, *13*(7), 868–872.

927 Jeffery, K. J., Jovalekic, A., Verriotis, M., & Hayman, R. (2013). Navigating in a three-
928 dimensional world. *Behavioral and Brain Sciences*, *36*(5), 523–543.

929 Johnson, A., & Redish, A. D. (2007). Neural ensembles in CA3 transiently encode paths

930 forward of the animal at a decision point. *The Journal of Neuroscience*, *27*(45), 12176–
931 12189.

932 Kempter, R., Leibold, C., Buzsaki, G., Diba, K., & Schmidt, R. (2012). Quantifying circular-
933 linear associations: Hippocampal phase precession. *Journal of Neuroscience Methods*,
934 *207*, 113–124.

935 Knierim, J. J., & Hamilton, D. A. (2011). Framing spatial cognition: neural representations of
936 proximal and distal frames of reference and their roles in navigation. *Physiological*
937 *Reviews*, *91*, 1245–1279.

938 Knierim, J. J., Kudrimoti, H. S., & McNaughton, B. L. (1998). Interactions between
939 idiothetic cues and external landmarks in the control of place cells and head direction
940 cells. *Journal of Neurophysiology*, *80*(1), 425–446.

941 Knierim, J. J., & McNaughton, B. L. (2001). Hippocampal place-cell firing during movement
942 in three-dimensional space. *Journal of Neurophysiology*, *85*, 105–116.

943 Komorowski, R. W., Manns, J. R., & Eichenbaum, H. (2009). Robust conjunctive item-place
944 coding by hippocampal neurons parallels learning what happens where. *The Journal of*
945 *Neuroscience*, *29*(31), 9918–9929.

946 Leutgeb, S., Leutgeb, J. K., Barnes, C. A., Moser, E. I., McNaughton, B. L., & Moser, M.-B.
947 (2005). Independent codes for spatial and episodic memory in hippocampal neuronal
948 ensembles. *Science*, *309*(5734), 619–23.

949 Leutgeb, S., Leutgeb, J. K., Treves, A., Moser, M.-B., & Moser, E. I. (2004). Distinct
950 Ensemble Codes in Hippocampal Areas CA3 and CA1. *Science*, *305*(5688), 1295–1298.

951 Lever, C., Burton, S., Jeewajee, A., O'Keefe, J., & Burgess, N. (2009). Boundary Vector
952 Cells in the Subiculum of the Hippocampal Formation. *The Journal of Neuroscience*,

953 *29*(31), 9771–9777.

954 Mamad, O., Stumpp, L., McNamara, H. M., Ramakrishnan, C., Deisseroth, K., Reilly, R. B.,
955 & Tsanov, M. (2017). Place field assembly distrivution encodes preffered locations.
956 *PLOS Biology, 15*(9): e2002365.

957 Margaria, R., Cerretelli, P., Aghemo, P., & Sassi, G. (1963). Energy cost of running. *Journal*
958 *of Applied Physiology*, *18*(2), 367–370.

959 McKenzie, S., Frank, A. J., Kinsky, N. R., Porter, B., Rivière, P. D., & Eichenbaum, H.
960 (2014). Hippocampal representation of related and opposing memories develop within
961 distinct, hierarchically organized neural schemas. *Neuron*, *83*(1), 202–215.

962 McNaughton, B. L., Battaglia, F. P., Jensen, O., Moser, E. I., & Moser, M.-B. (2006). Path
963 integration and the neural basis of the "cognitive map." *Nature Reviews Neuroscience*,
964 *7*(8), 663–678.

965 Miao, C., Cao, Q., Ito, H. T., Yamahachi, H., Witter, M. P., Moser, M. B., & Moser, E. I.
966 (2015). Hippocampal remapping after partial inactivation of the medial entorhinal
967 cortex. *Neuron*, *88*(3), 590–603.

968 Minetti, A. E., Moia, C., Roi, G. S., Susta, D., & Ferretti, G. (2002). Energy cost of walking
969 and running at extreme uphill and downhill slopes. *Journal of Applied Physiology*, *93*,
970 1039–1046.

971 Muller, R. U., & Kubie, J. L. (1987). The effects of changes in the environment on the spatial
972 firing of hippocampal comples-spike cells. *The Journal of Neuroscience*, *7*(7), 1951–
973 1968.

974 Muller, R. U., & Kubie, J. L. (1989). The firing of hippocampal place cells predicts the future
975 position of freely moving rats. *The Journal of Neuroscience*, *9*(12), 4101–4110.

976 Naismith, W. W. (1892). Cruach Ardran, Stobinian, and Ben More. *Scottish Mountaineering*
977 *Club Journal*, *2*(3).

978 Navawongse, R., & Eichenbaum, H. (2013). Distinct pathways for rule-based retrieval and
979 spatial mapping of memory representations in hippocampal neurons. *The Journal of*
980 *Neuroscience*, *33*(3), 1002–1013.

981 O'Keefe, J., & Dostrovsky, J. (1971). The hippocampus as a spatial map. Preliminary
982 evidence from unit activity in the freely-moving rat. *Brain Research*, *34*, 171–175.

983 O'Keefe, J., & Nadel, L. (1978). *The hippocampus as a cognitive map*. Oxford University
984 Press.

985 O'Keefe, J., & Recce, M. L. (1993). Phase relationship between hippocampal place units and
986 the EEG theta rhythm. *Hippocampus*, *3*(3), 317–330.

987 Ormond, J., & McNaughton, B. L. (2015). Place field expansion after focal MEC
988 inactivations is consistent with loss of Fourier components and path integrator gain
989 reduction. *Proceedings of the National Academy of Sciences*, *112*(13), 201421963.

990 Paxinos, G., & Watson, C. (2007). *The Rat Brain in Stereotaxic Coordinates* (Sixth). San
991 Diego: Elsevier.

992 Pfeiffer, B. E., & Foster, D. J. (2013). Hippocampal place-cell sequences depict future paths
993 to remembered goals. *Nature*, *497*(7447), 74–9.

994 Preston, A. R., & Eichenbaum, H. (2013). Interplay of hippocampus and prefrontal cortex in
995 memory. *Current Biology*, *23*(17), 764–773.

996 Proffitt, D. R., Stefanucci, J., Banton, T., & Epstein, W. (2003). The role of effort in
997 perceiving distance. *Psychological Science*, *14*, 106–112.

998 Pursky, G. T., Harker, K. T., Douglas, R. M., and Whishaw, I. Q. (2002) Variation in visual
999 acuity within pigmented, and between pigmented and albino rat strains. *Behavioural*
1000 *Brain Research, 1236*(2): 339 – 348.

1001 Remondes, M., & Wilson, M. A. (2013). Cingulate-hippocampus coherence and trajectory
1002 coding in a sequential choice task. *Neuron*, *80*(5), 1277–1289.

1003 Remondes, M., & Wilson, M. A. (2015). Slow-γ rhythms coordinate cingulate cortical
1004 responses to hippocampal sharp-wave ripples during wakefulness. *Cell Reports*, *13*(7),
1005 1327–1335.

1006 Rueckemann, J. W., Dimauro, A. J., Rangel, L. M., Han, X., Boyden, E. S., & Eichenbaum,
1007 H. (2016). Transient optogenetic inactivation of the medial entorhinal cortex biases the
1008 active population of hippocampal neurons. *Hippocampus*, *26*(2), 246–260.

1009 Russell, N. A., Horii, A., Smith, P. F., Darlington, C. L., & Bilkey, D. K. (2003). Long-term
1010 effects of permanent vestibular lesions on hippocampal spatial firing. *The Journal of*
1011 *Neuroscience*, *23*(16), 6490–6498.

1012 Savelli, F., & Knierim, J. J. (2010). Hebbian analysis of the transformation of medial
1013 entorhinal grid-cell inputs to hippocampal place fields. *Journal of Neurophysiology*,
1014 *103*(6), 3167–3183.

1015 Savelli, F., & Knierim, J. J. (2011). Coming up: in search of the vertical dimension in the
1016 brain. *Nature Neuroscience*, *14*(9), 1102–1103.

1017 Scarf, P. (2007). Route choice in mountain navigation, Naismith's rule, and the equivalence
1018 of distance and climb. *Journal of Sports Sciences*, *25*(6), 719–726.

1019 Shen, J., Barnes, C. A., Mcnaughton, B. L., Skaggs, W. E., & Weaver, K. L. (1997). The
1020 effect of aging on experience-dependent plasticity of hippocampal place cells. *The*

Journal of Neuroscience, *17*(17), 6769–6782.

Singer, A. C., Carr, M. F., Karlsson, M. P., & Frank, L. M. (2013). Hippocampal SWR Activity Predicts Correct Decisions during the Initial Learning of an Alternation Task. *Neuron*, *77*(6), 1163–1173.

Skaggs, W. E., Mcnaughton, B. L., Gothard, K. M., & Markus, E. J. (1993). An information-theoretic approach to deciphering the hippocampal code. *Advances in Neural Information Processing Systems*, *5*(1990), 1030–1037.

Skaggs, W. E., McNaughton, B. L., Wilson, M. A., & Barnes, C. A. (1996). Theta phase precession in hippocampal neuronal populations and the compression of temporal sequences. *Hippocampus*, *6*(2), 149–172.

Smith, D. M., & Mizumori, S. J. Y. (2006). Hippocampal place cells, context, and episodic memory. *Hippocampus*, *16*, 716–729.

Smith, P. F. (1997). Vestibular-hippocampal interactions. *Hippocampus*, *7*(5), 465–471.

Smith, P. F., Horii, A., Russell, N., Bilkey, D. K., Zheng, Y., Liu, P., … Darlington, C. L. (2005). The effects of vestibular lesions on hippocampal function in rats. *Progress in Neurobiology*, *75*(6), 391–405.

Stackman, R. W., Clark, A. S., & Taube, J. S. (2002). Hippocampal spatial representations require vestibular input. *Hippocampus*, *12*(3), 291–303.

Stackman, R. W., & Taube, J. S. (1997). Firing properties of head direction cells in the rat anterior thalamic nucleus: dependence on vestibular input. *The Journal of Neuroscience*, *17*(11), 4349–58.

Stackman, R. W., & Taube, J. S. (1998). Firing properties of rat lateral mammillary single units: head direction, head pitch, and angular head velocity. *The Journal of*

1044 *Neuroscience*, *18*(21), 9020–37.

1045 Stefanucci, J. K., Proffitt, D. R., Banton, T., & Epstein, W. (2005). Distances appear different
1046 on hills. *Perception & Psychophysics*, *67*(6), 1052–60.

1047 Taube, J. S. (1998). Head direction cells and the neurophysiological basis for a sense of
1048 direction. *Progress in Neurobiology*, *55*(3), 225–256.

1049 Taube, J. S., Muller, R. U., & Ranck, J. B. (1990). Head-direction cells recorded from the
1050 postsubiculum in freely moving rats. I. Description and quantitative analysis. *The*
1051 *Journal of Neuroscience* , *10*(2), 420–435.

1052 Taube, J. S., & Shinder, M. (2013). On the nature of three-dimensional encoding in the
1053 cognitive map: Commentary on Hayman, Verriotis, Jovalekic, Fenton, and Jeffery.
1054 *Hippocampus*, *23*, 14–21.

1055 Terrazas, A., Krause, M., Lipa, P., Gothard, K. M., Barnes, C. A., & McNaughton, B. L.
1056 (2005). Self-Motion and the Hippocampal Spatial Metric. *The Journal of Neuroscience*,
1057 *25*(35), 8085–8096.

1058 Ulanovsky, N. (2011). Neuroscience: How is three-dimensional space encoded in the brain?
1059 *Current Biology*, *21*(21), R886–R888.

1060 Ulanovsky, N., & Moss, C. F. (2007). Hippocampal cellular and network activity in freely
1061 moving echolocating bats. *Nature Neuroscience*, *10*(2), 224–233.

1062 Wall, J., Douglas-Hamilton, I., & Vollrath, F. (2006). Elephants avoid costly mountaineering.
1063 *Current Biology*, *16*(14), 527–529.

1064 Wallace, D. G., Hines, D. J., Pellis, S. M., & Whishaw, I. Q. (2002). Vestibular information
1065 is required for dead reckoning in the rat. *The Journal of Neuroscience*, *22*(22), 10009–
1066 10017.

1067 Wiener, S. I., Korshunov, V. A., Garcia, R., & Berthoz, A. (1995). Inertial, substratal and
1068 landmark cue control of hippocampal ca1 place cell activity. *European Journal of*
1069 *Neuroscience*, *7*(11), 2206–2219.

1070 Wikenheiser, A. M., & Redish, A. D. (2015). Hippocampal theta sequences reflect current
1071 goals. *Nature Neuroscience*, *18*(2) 289 - 294.

1072 Witt, J. K., Proffitt, D. R., & Epstein, W. (2004). Perceiving distance: A role of effort and
1073 intent. *Perception*, *33*, 577–590.

1074 Yartsev, M. M., & Ulanovsky, N. (2013). Representation of three-dimensional space in the
1075 hippocampus of flying bats. *Science*, *340*, 367–372.

1076 Zar, J. H. (1999). Two-sample and multisample testing of mean angles. In *Biostatistical*
1077 *Analysis* (4th ed., pp. 625–630). Upper Saddle River: Prentice Hall.

1078 Zinyuk, L., Kubik, S., Kaminsky, Y., Fenton, A. A., & Bures, J. (2000). Understanding
1079 hippocampal activity by using purposeful behavior: place navigation induces place cell
1080 discharge in both task-relevant and task-irrelevant spatial reference frames. *Proceedings*
1081 *of the National Academy of Sciences of the United States of America*, *97*(7), 3771–3776.

1082

Figure 1

a

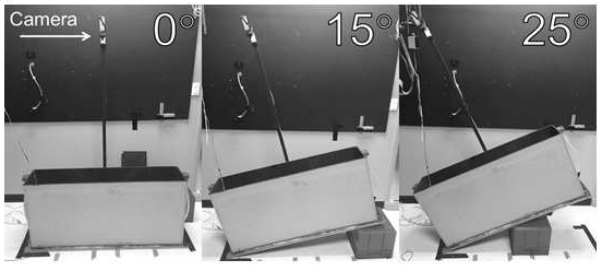

b

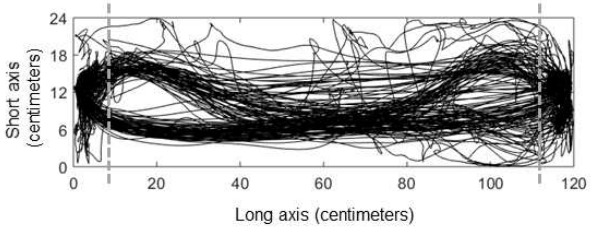

c

	Tilt condition presentation order		
Day 1	Flat, 0°	North, 15°	North, 25°
Day 2	North, 15°	North, 25°	Flat, 0°
Day 3	North, 25°	Flat, 0°	North, 15°
Day 4	South, 15°	Flat, 0°	South, 25°
Day 5	Flat, 0°	South, 25°	South, 15°
Day 6	South, 25°	South, 15°	Flat, 0°

d

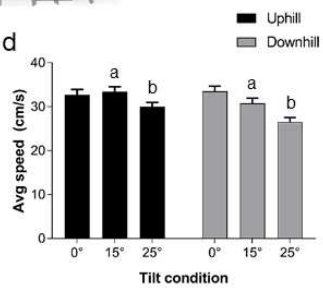

Tilt: F(2,74) = 19.88****
Slope direction: F(1,37) = 9.90***
Interaction: F(2,74) = 10.33****

e

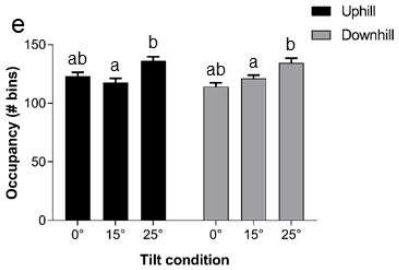

F(2,74) = 13.51****
F(1,37) = 0.82$^{n.s.}$
F(2,74) = 2.42$^{n.s.}$

Figure 2

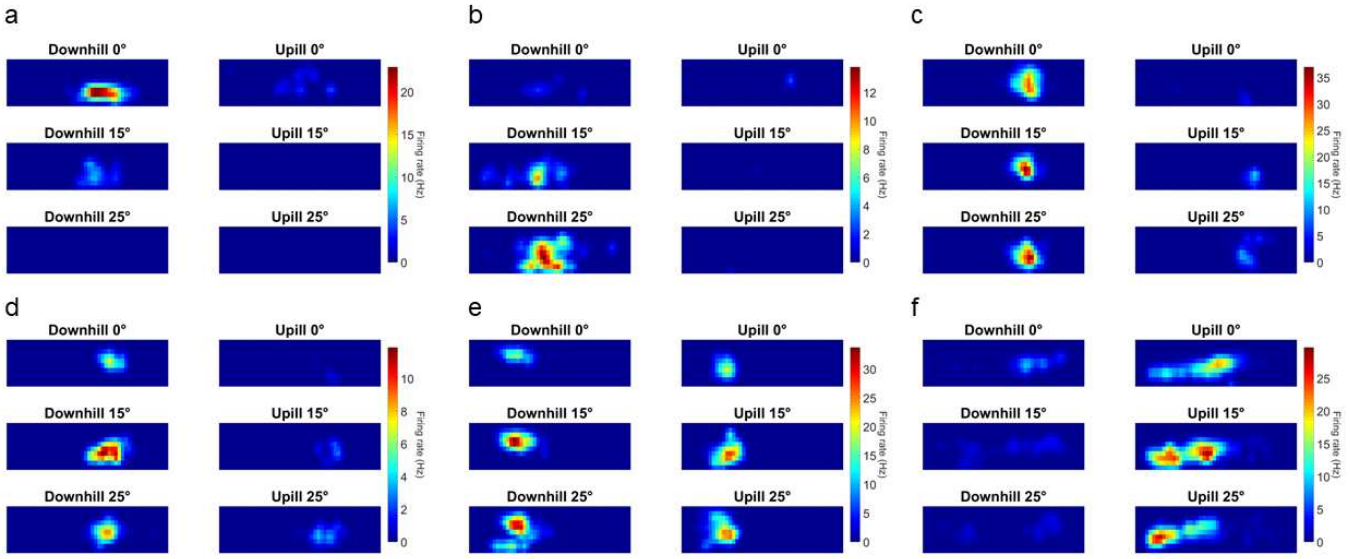
a
Downhill 0°
Upill 0°
Downhill 15°
Upill 15°
Downhill 25°
Upill 25°
20
15
10
5
0
Firing rate (Hz)
b
Downhill 0°
Upill 0°
Downhill 15°
Upill 15°
Downhill 25°
Upill 25°
12
10
8
6
4
2
0
Firing rate (Hz)
c
Downhill 0°
Upill 0°
Downhill 15°
Upill 15°
Downhill 25°
Upill 25°
35
30
25
20
15
10
5
0
Firing rate (Hz)
d
Downhill 0°
Upill 0°
Downhill 15°
Upill 15°
Downhill 25°
Upill 25°
10
8
6
4
2
0
Firing rate (Hz)
e
Downhill 0°
Upill 0°
Downhill 15°
Upill 15°
Downhill 25°
Upill 25°
30
25
20
15
10
5
0
Firing rate (Hz)
f
Downhill 0°
Upill 0°
Downhill 15°
Upill 15°
Downhill 25°
Upill 25°
25
20
15
10
5
0
Firing rate (Hz)

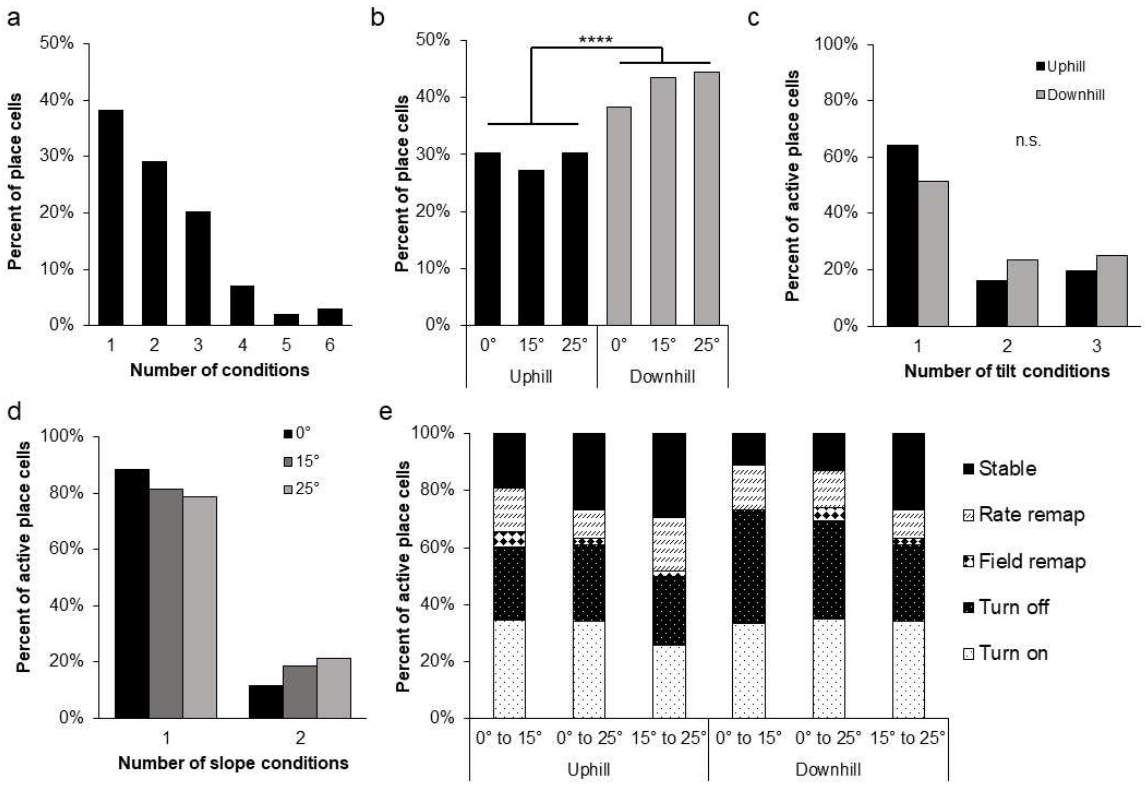
a
Percent of place cells
50%
40%
30%
20%
10%
0%
1 2 3 4 5 6
Number of conditions
b
Percent of place cells
****
0° 15° 25° 0° 15° 25°
Uphill
Downhill
c
Percent of active place cells
Uphill
Downhill
n.s.
1 2 3
Number of tilt conditions
d
Percent of active place cells
0°
15°
25°
1 2
Number of slope conditions
e
Percent of active place cells
0° to 15° 0° to 25° 15° to 25° 0° to 15° 0° to 25° 15° to 25°
Uphill
Downhill
Stable
Rate remap
Field remap
Turn off
Turn on

Figure 3

Figure 4

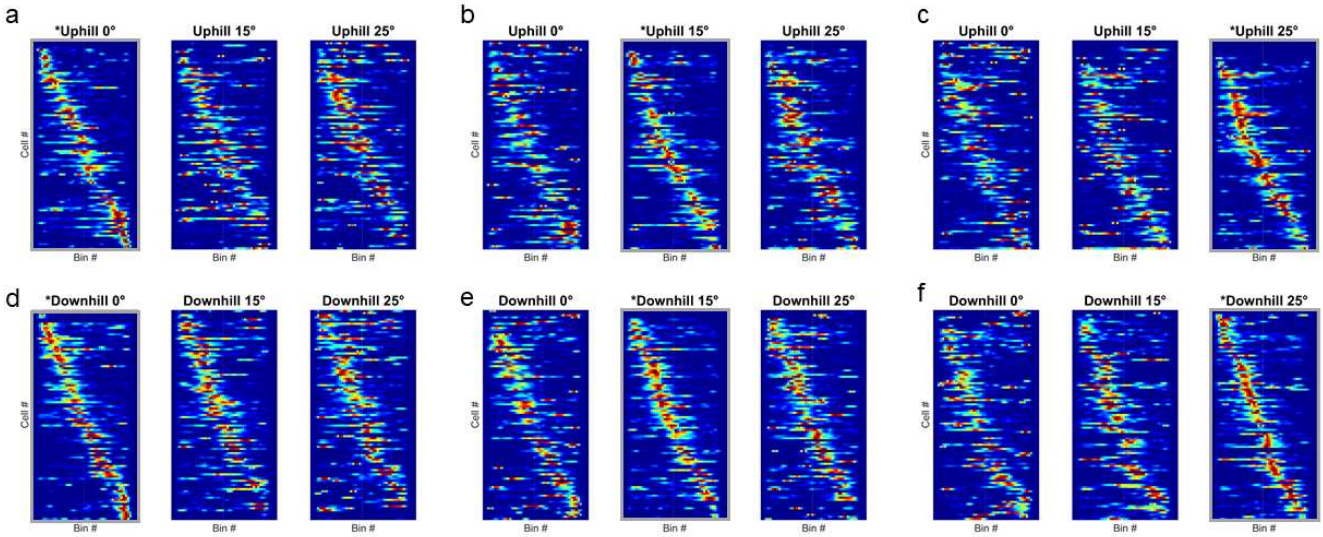
a
*Uphill 0°
Uphill 15°
Uphill 25°
b
Uphill 0°
*Uphill 15°
Uphill 25°
c
Uphill 0°
Uphill 15°
*Uphill 25°
d
*Downhill 0°
Downhill 15°
Downhill 25°
e
Downhill 0°
*Downhill 15°
Downhill 25°
f
Downhill 0°
Downhill 15°
*Downhill 25°
Cell #
Bin #

Figure 5

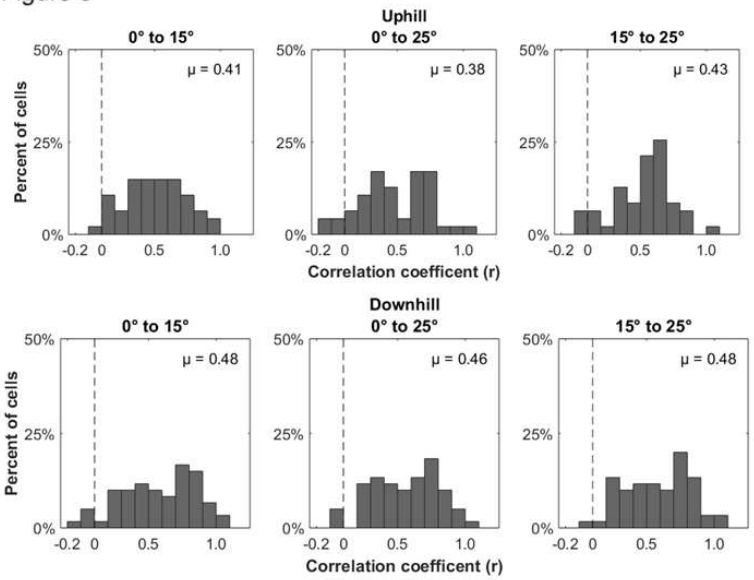

Slope direction: $F(1, 285) = 3.51^{n.s.}$
Angle difference: $F(2,285) = 0.89^{n.s.}$
Interaction: $F(2,285) = 0.95^{n.s.}$

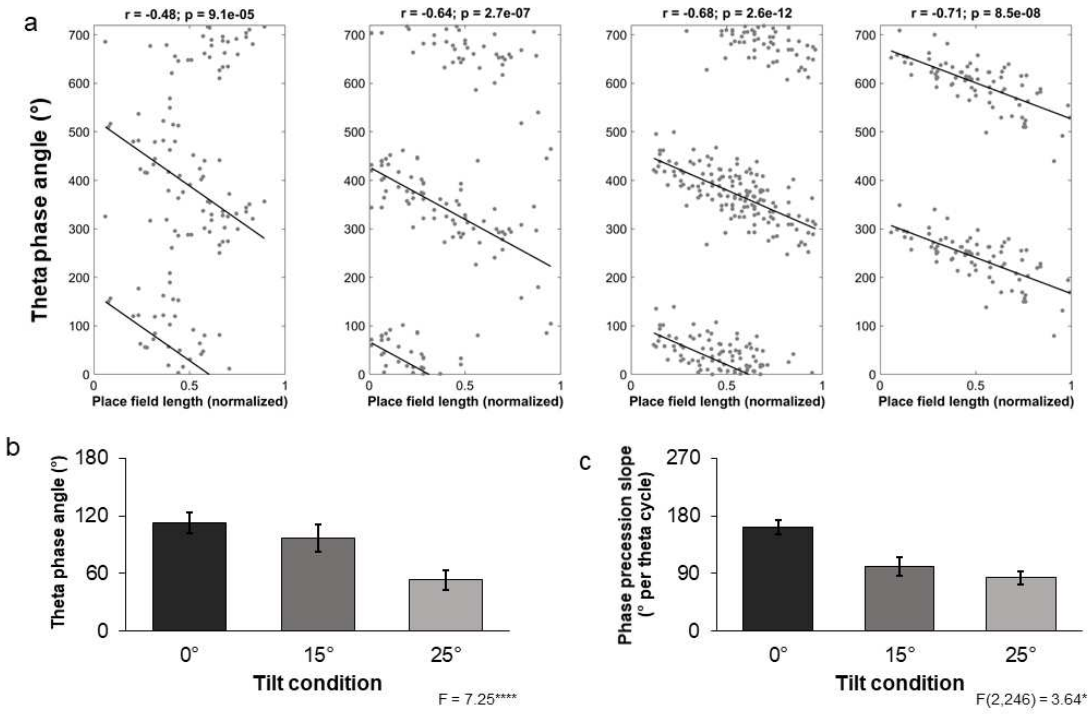
a
r = -0.48; p = 9.1e-05
r = -0.64; p = 2.7e-07
r = -0.68; p = 2.6e-12
r = -0.71; p = 8.5e-08
Theta phase angle (°)
Place field length (normalized)
b
Theta phase angle (°)
Tilt condition
0°
15°
25°
F = 7.25****
c
Phase precession slope (° per theta cycle)
Tilt condition
F(2,246) = 3.64*

Figure 6

	Uphill			Downhill		
	0°	15°	25°	0°	15°	25°
Firing rate (Hz)	3.31±0.25	3.63±0.37	3.58±0.38	3.81±0.26	3.64±0.33	3.23±0.25
Peak firing rate (Hz)	32.7±2.4	33.5±3.4	36.6±3.2	33.7±2.3	36.5±2.7	35.4±2.5
Information score (bits/spk)	1.62±0.08	1.57+±0.07	1.68±0.06	1.62±0.07	1.72±0.08	1.71±0.07
Sparsity*	0.24±0.01	0.25±0.01	0.22±0.01	0.25±0.01	0.23±0.01	0.22±0.01
Spatial coherence (r)	0.90±0.04	0.98±0.05	0.94±0.05	1.10±0.06	1.01±0.05	0.94±0.04
Number of place fields	1.30±0.10	1.33±0.12	1.23±0.08	1.21±0.07	1.21±0.06	1.25±0.07
Total fields / occupancy (%)	27%±2%	24%±2%	26%±1%	24%±1%	24%±1%	23%±2%
Main field / occupancy (%)	26%±2%	22%±1%	25%±2%	23%±2%	23%±1%	22%±1%
Place field aspect ratio	3.23±0.32	3.13±0.33	3.09±0.40	3.31±0.23	2.89±0.16	2.85±0.17
Infield firing rate (Hz)	12.4±1.26	14.2±2.01	14.1±1.33	15.0±1.31	15.8±1.53	14.2±1.34
Outfield firing rate (Hz)	1.08±0.11	1.32±0.14	1.18±0.15	1.18±0.09	1.16±0.13	1.13±0.10

Table 1: Place cell metrics across tilt-slope direction conditions. * indicates significant effect ($P < 0.05$) for tilt or slope direction (see text for details).

	Top	Bottom
Inactive	44	45
Turn on	17	24
Turn off	24	11
Field remap	3	2
Rate remap	4	7
Stable	6	11

Table 2: Frequency of remapping types observed in place cells between 0° and tilt conditions (15° and 25°) based on main place field location within the apparatus.

	Within	Between
Inactive	379	228
Turn on	36	60
Turn off	55	45
Field remap	4	4
Rate remap	13	10
Stable	107	49

Table 3: Frequency of remapping types observed in place cells between 0° and tilt conditions (15° and 25°) based on main place field location within the apparatus.